Schalbetter, S. A., Mansoubi, S., Chambers, A., Downs, J. A., & Baxter, J. (2015). Fork rotation and DNA pre-catenation is restricted during DNA replication to prevent chromosomal instability. *Proceedings of the National Academy of Sciences of the United States of America*, *112*(33), E4565–E4570. https://doi.org/10.1073/pnas.1505356112

Classification: **Biological Sciences; Genetics**

Fork rotation and DNA pre-catenation is restricted during DNA replication to prevent chromosomal instability

Short title: Replication fork rotation in eukaryotes

S. A. Schalbetter[1], S. Mansoubi[1], A. L. Chambers[12], J. A. Downs[1] and J. Baxter[1*]

Affiliations:

[1] Genome Damage and Stability Centre, Science Park Road, University of Sussex, Falmer, Brighton, East Sussex BN1 9RQ, U.K.

[2] School of Biochemistry, University of Bristol, Bristol BS8 1TD, U.K.

*Correspondence to:

Jonathan Baxter

Genome Damage and Stability Centre,

Science Park Road, University of Sussex,

Falmer, Brighton, East Sussex BN1 9RQ, U.K.

Email: Jon.Baxter@sussex.ac.uk

Tel: +44 (0)1273 876637

Key words:

Genome integrity, DNA replication, catenation, topology, fragile sites

Abstract

Faithful genome duplication and inheritance requires the complete resolution of all intertwines within the parental DNA duplex. This is achieved by topoisomerase action ahead of the replication fork or by fork rotation and subsequent resolution of the DNA pre-catenation formed. Although fork rotation predominates at replication termination, *in vitro* studies have suggested that it also occurs frequently during elongation. However, the factors that influence fork rotation and how rotation and pre-catenation may influence other replication associated processes are unknown. Here we analyze the causes and consequences of fork rotation in budding yeast. We find that fork rotation and pre-catenation preferentially occurs in contexts that inhibit unwinding, including stable protein-DNA fragile sites and termination. However, although fork rotation is induced by these local contexts, generally fork rotation and pre-catenation is actively prevented by Timeless/Tof1 and Tipin/Csm3. In unperturbed cells fork rotation and pre-catenation causes extensive DNA damage following DNA replication. In unperturbed cells, damage related to fork rotation is limited to the fragile protein-DNA sites where pre-catenation occurs. We conclude that although fork rotation and pre-catenation facilitates unwinding in hard to replicate contexts, it intrinsically disrupts normal chromosome duplication and is therefore restricted by Timeless/Tipin.

Significance Statement

Genome inheritance requires the complete resolution of all intertwines within parental DNA. This is facilitated by fork rotation and pre-catenation of the newly replicated DNA. However, the general importance and frequency of fork rotation *in vivo* is poorly understood. We find that the evolutionarily conserved Timeless and Tipin proteins actively inhibit fork rotation in budding yeast. In their presence fork rotation appears restricted to hard to replicate fragile sites. In their absence excessive fork rotation leads to damage accumulating in the replicated sister chromatids especially at known yeast fragile sites. Therefore fork rotation appears to be restricted to contexts where it is absolutely required for unwinding and that this restriction is required to prevent pre-catenation inducing excessive chromosomal fragility.

\body

Introduction

During DNA replication it is essential to completely unwind and remove all the intertwining between the two strands of the template DNA double helix. This is achieved by the combined action of replicative helicases and topoisomerases. During elongation replicative helicases force the strands apart, generating compensatory topological overwinding stress in the unreplicated region ahead of the fork. If overwinding accumulates it prevents further DNA replication (1, 2). Relaxation of the stress is achieved either by topoisomerase action ahead of the fork, directly on the overwound region, or by coupling helicase action with rotation of the whole fork relative to the unreplicated DNA (*SI Appendix*, Fig. S1). This latter pathway relaxes topological stress ahead of the fork at the expense of generating double stranded intertwines behind the fork, often referred to as DNA pre-catenanes (3, 4). These intertwines are subsequently resolved by the action of type II topoisomerases. If type II topoisomerases do not completely resolve either the pre-catenanes or the full DNA catenanes formed at the completion of replication the unresolved intertwines will cause chromosome bridging, non-disjunction and aneuploidy (5). Fork rotation and DNA pre-catenation appears to be the primary pathway of unlinking when forks come together at the termination of DNA replication (6, 7). In addition, *in vitro,* fork rotation appears to be a frequent event during elongation; it can support ongoing replication, and extensive pre-catenation is observed behind elongating forks (8-10). Therefore the prevailing view is that the topological stress caused by DNA unwinding is resolved stochastically during elongation by both topoisomerase action ahead of the fork and fork rotation and DNA decatenation behind the fork (3, 11). At termination the diminishing distance between converging replisomes is thought to prevent topoisomerase action ahead of the fork, leaving fork rotation as the primary pathway for DNA unwinding in this

context. However, unlike viral replisomes and replication complexes established in *in vitro* systems, the eukaryotic replisome holo-enzyme is composed of a far greater number of proteins and activities. These factors are thought to facilitate replication through the highly variable eukaryotic genomic landscape and co-ordinate lagging strand synthesis with other chromatid maturation processes such as chromatin assembly and cohesion establishment (5). These latter processes act on the same newly replicated DNA potentially braided by pre-catenation. How these processes occurring in the wake of the fork may be impeded by the formation of pre-catenation is unexplored (5).

In order to study these events *in vivo* we have directly examined fork rotation and pre-catenation in budding yeast. We show that fork rotation and pre-catenation is not stochastic but rather is actively restricted to distinct contexts by the evolutionarily conserved homologues of Timeless/Tipin, Tof1/Csm3. Failure to regulate fork rotation leads to significantly elevated levels of DNA damage, particularly at known fragile sites. Therefore the eukaryotic replisome appears to minimize rotation and pre-catenation, so that it is utilized to unwind DNA only when absolutely necessary to maintain genome stability.

Results

Fork rotation during replication elongation is not stochastic and is restricted to distinct genomic contexts.

To assess fork rotation *in vivo* we adapted a previously described plasmid DNA catenation assay for use with yeast episomal plamids (12, 13). The conditional loss of type II topoisomerase activity during DNA replication leads to the accumulation of catenated replicated plasmids in yeast (14), due to the DNA pre-catenanes formed through fork rotation not being resolved by Top2. Assaying the extent of DNA

catenation on these plasmids by agarose gel electrophoresis allows a direct assessment of the frequency of formation of pre-catenation and therefore fork rotation (assay fully outlined in *SI Appendix*, Fig. S2). To conditionally remove topoisomerase II activity from cells specifically during DNA replication, we synchronized the *top2-4* yeast strain (15) in G1, switched the cells to the restrictive temperature to ablate Top2 activity and then released them into the cell cycle, allowing plasmid replication and formation of catenated sister chromatids. For analysis we then purified DNA following replication without Top2, nicked the plasmids with a site specific nuclease and then resolved and quantified the entire distribution of relaxed and catenated plasmids (referred to as CatAn where n = number of catenated linkages), by two dimensional gel electrophoresis, Southern blotting and densitometry. Using this assay we found that replication of the 5kb yeast ARS/CEN episomal plasmid pRS316 produced a normal distribution of catenated states with a median of 13. Analysis of the tail of the distribution indicated that 14% of the population appeared highly catenated (i.e. with plasmids containing more than 20 catenations (CatAn >20)) (Fig. 1A). Bacterial *Topo III* can resolve pre-catenation in vitro by acting on gaps in the lagging strand (8). To eliminate the possibility that the activity of yeast Top3 may have led to an underestimation of fork rotation, we assessed DNA catenation of the plasmid in the absence of both Top2 and Top3. However, we did no observe any significant difference in DNA catenation of pRS316 in the absence of Top3 and Top2 compared to Top2 alone (*SI Appendix*, Fig. S3A), indicating that Top3 does not resolve pre-catenanes in this context. Finally, to test if residual Top2 activity in the *ts* allele could be modifying our results we compared catenated plasmids generated immediately following DNA replication with catenated plasmids maintained a further hour in a post-replicative block. No residual decatenation activity could be detected (*SI Appendix*, Fig. S3B). Therefore

we conclude that our analysis of DNA catenation is providing a direct assessment of fork rotation and pre-catenation on these replicons.

If fork rotation occurs stochastically during elongation, increasing the size of a replicon should increase the incidence of fork rotation during its replication. To assay if increasing the size of the replicon led to increased fork rotation we first ligated 3kb of DNA into pRS316, increasing the size of the plasmid by 60%. However, no difference in the distribution of DNA catenation was observed (median n=12, 14% of plasmids had > 20 catenations) (Fig. 1B). We then ligated a further 4kb of DNA into the plasmid increasing the size of the replicon to by 140% (to 12kb) and re-analyzed DNA catenation. On this plasmid we observed a spreading of the distribution of catenated states, compared to the smaller plasmids, but did not see an increase of the median of the population (median n=13, 21% of plasmids had > 20 catenations) (Fig. 1C). Therefore, *in vivo,* increasing the size of the plasmid replicon does not significantly alter the overall extent of DNA catenation, indicating that elongation distance is not the primary determinant of the extent of fork rotation during DNA replication. Rather our data suggests that the extent of fork rotation is regulated by distinct contexts within the replicon such as the termination of DNA replication.

Fork rotation is predicted to be more frequent at termination because the convergence of two replisomes spatially restricts topoisomerase access to the unreplicated DNA between them (11). In this model the replisomes have to rotate in order to unwind the final few turns of DNA (Fig. 1D left). Projecting this model onto the different chromosomal contexts of DNA replication we postulated that a similar situation would arise when the fork passes through stable protein-DNA complexes that are known to pause ongoing replication (16) (Fig. 1D right). When the fork

approaches a stable protein-DNA complex that pauses replication, topoisomerases will be spatially inhibited from accessing the DNA between the encroaching replisome and the stable complex, potentially requiring fork rotation to allow ongoing replication. To test this hypothesis we assessed if pausing structures in plasmid replicons led to increased fork rotation during replication. We compared similar sized plasmids that contained either; no known pause site (pRS426), a point centromere pause site (pRS316) or multiple pausing sites consisting of 3 tRNA genes and a centromere (tRNApRS316). Catenation analysis of pRS426, produced a slightly reduced distribution of catenated states compared to the one pause site plasmid pRS316, with pRS426 (median n=12, 8% of plasmids with > 20 catenations) (Fig. 1E). In contrast a substantial increase in catenation was observed for the multiple pause site plasmid tRNApRS316 (median n=16, 28% of plasmids had > 20 catenations) (Fig. 1F). Therefore replication through tRNAs and potentially centromeres increases fork rotation and DNA catenation over and above the catenation that occurs at termination. We extended our analysis to inactive origins, where DNA-bound ORC and MCM proteins pause replication (16). We achieved this by comparing a 7 origin plasmid to a 1 origin plasmid (17). On multi-origin plasmids, only 1 origin is activated and the remaining inactive origins are passively replicated (18). The 7 origin plasmid based on the YIPlac plasmid became highly catenated during DNA replication (median n=16, 35% of plasmids with > 20 catenations) compared to a YIPlac plasmid containing 1 copy of the origin (median n=12 with 12% of plasmids with > 20 catenations) (Fig. 1H, G) (full summary of DNA catenation experiments in *SI Appendix*, Table S2). Together these data argue that replication through stable structures that pause DNA replication including tRNAs, inactive origins and potentially centromeres (16) induces fork rotation and pre-catenation during replication elongation.

Timeless/Tof1 and Tipin/Csm3 restrict fork rotation

Since stable protein-DNA complexes both pause replication and cause fork rotation, we next examined if factors that influence fork pausing also alter fork rotation. Deletion of the *Timeless* homologue *TOF1* leads to reduced pausing at stable protein-DNA complexes (19). Therefore we examined if deletion of *TOF1* alters fork rotation during replication of plasmid pRS316. In *tof1Δ* cells we observed a radical increase in the number of DNA catenanes formed on the plasmid. The distribution of highly catenated states was dramatically shifted, with a median in excess of 30 (64% of the distribution containing > 30 catenanes) (Fig. 2A). Therefore Tof1 appears to restrict fork rotation during DNA replication on this replicon. We then examined how deletion of other replisome factors linked to Tof1/Timeless altered fork rotation on pRS316. Excessive fork rotation was also observed in cells deleted for the yeast homologue of Tipin, *CSM3*, the conserved partner of Tof1/Timeless in the replisome (20) (Fig. 2B). Claspin/Mrc1 and AND1/Ctf4 have also been reported to be linked to Tof1/Csm3 function (21, 22). However, neither deletion of *MRC1* or *CTF4* increased fork rotation during replication of the plasmid (Figure 2C, *SI Appendix*, Fig. S4). We also examined the potential role of the protein displacement helicase *RRM3* on fork rotation. Rrm3 is required *in vivo* to minimize fork pausing at stable protein-DNA structures, presumably by promoting their displacement to allow rapid replication passage (16). Deletion of *RRM3* produced a significant increase in fork rotation on plasmid pRS316 (Fig. 2D), however this increase appeared modest compared to *tof1Δ* or *csm3Δ* cells. We conclude that *TOF1/CSM3* and *RRM3* are involved in distinct pathways to inhibit fork rotation *in vivo*.

We next examined the effects on fork rotation of deleting either *RRM3* or *TOF1* on plasmids with and without pause sites. We observed that deletion of *RRM3* increased fork rotation only on plasmids containing pause sites (Fig. 3A, B when

compared to Fig. 1E, F, *SI Appendix*, Table S2). This suggests that Rrm3 is required to rapidly displace stable protein-DNA complexes and allows accelerated access of topoisomerases ahead of the fork, limiting the need for fork rotation at such sites (*SI Appendix*, Fig. S5). In contrast, we observed that deletion of *TOF1* caused hyper-catenation of plasmids irrespective of the number of pause sites (Figure 3C, D). This suggests that Tof1/Csm3 more generally restricts fork rotation during DNA replication and not just at pause sites. Deletion of TOF1/Timeless is reported to slow replisome elongation rates (23). Potentially excessive fork rotation in *tof1/csm3* cells could be due to slower elongation, which could hypothetically favor fork rotation. However, we did not detect any increase in DNA catenation occurring on plasmids replicated either in the presence of hydroxyurea, which would be predicted to arrest fork progression (*SI Appendix*, Fig. S6A), or in cells deleted for the leading strand polymerase elongation factor *DPB3* (*SI Appendix*, Fig. S6B) which causes a general slowing of DNA replication (*SI Appendix*, Fig. S6C). Therefore unrestricted fork rotation does not appear to be a consequence of general fork slowing but rather is directly related to Tof1/Csm3 function.

Unrestricted fork rotation and DNA catenation causes aneuploidy and triggers a G2/M arrest in cells

We next sought to confirm that loss of Tof1 function leads to excessive DNA catenation on endogenous chromosomes. Consistent with excessive fork rotation and DNA catenation occurring in the absence of Tof1, *tof1Δ* cells were acutely sensitive to a partial reduction in Top2 activity induced by transcriptional repression of the *top2-td* allele (Fig. 4A). We next examined the extent of chromosome mis-segregation in cells where *TOF1* is deleted and Top2 either partially depleted (Fig. 4B) or wholly depleted (Fig. 4C). It has previously been shown in budding yeast that unresolved DNA catenation does not inhibit cell cycle progression but does cause

aneuploidy following cell division (14). If deletion of *TOF1* causes excessive DNA catenation then it would be predicted to cause aneuploidy at levels of Top2 activity that normally allow chromosome segregation. To test this prediction we first used semi-restrictive growth conditions that reduced Top2 dosage to a level just sufficient to allow normal segregation of endogenous chromosomes in a single cell cycle (Fig. 4B, left panel) with very few "cut" cells (indicative of gross mis-segregation (14)), cytologically observed (Fig. 4B, right panel). However, in the absence of *TOF1* this dosage of Top2 was not sufficient to prevent widespread mis-segregation of endogenous chromosomes and aneuploidy (Fig. 4B left panel) and "cut" cells were frequently observed in mitosis (Fig. 4B right panel). Therefore deletion of *TOF1* specifically sensitizes cells to partial loss of Top2, resulting in a phenotype that resembles a complete loss of Top2 (Fig. 4C). To control for the possibility that depleting Top2 in *tof1Δ* cells could also cause aneuploidy by general destabilization of the replisome, leading to frequent fork collapse, we repeated this set of experiments in *mrc1Δ cells.* Deletion of *MRC1,* destabilizes the replisome in response to replication stress in a similar manner to *tof1Δ* (21), but does not cause an increase in DNA catenation (Fig 2C). We observed that *mrc1Δ* cells are not as sensitive to partial loss of Top2 as *tof1Δ* cells (*SI Appendix*, Fig. S7A) and that deletion of *MRC1* does not cause the marked increase in "cut" nuclei observed following depletion of Top2 in *tof1Δ* cells (*SI Appendix*, Fig. S7B). These data indicate that the observed aneuploidy and mis-segregation observed in *tof1Δ* cells is not due to a general increase in fork arrest and collapse. Rather our observations are consistent with loss of *TOF1* leading to unrestricted fork rotation and formation of excessive DNA catenation on endogenous chromosomes.

Our plasmid analysis indicates that fork rotation is actively inhibited during DNA replication. This inhibition appears to be actively enforced through the cellular

function of Tof1/Csm3. This data raises the question of why fork rotation is actively inhibited? Fork rotation provides an important alternative pathway for unwinding since excessive fork rotation and the resultant DNA pre-catenation does not appear to be immediately lethal until Top2 becomes limiting. However, impaired Tof1/Timeless function leads to chronic genomic instability in cells. Increased levels of gross chromosomal rearrangements are observed in *tof1Δ* cells (24), whilst depletion of Timeless/Tipin orthologues in several systems causes constitutive DNA damage (20, 25). Potentially the chronic genome instability phenotypes and constitutive DNA damage of cells depleted for Tof1/Timeless could be directly linked to the abnormal excessive fork rotation and pre-catenation occurring during DNA replication. We reasoned that if the excessive fork rotation was leading to chronic genome instability, then such genome instability phenotypes should be exacerbated when Top2 is depleted since this would stabilize the pre-catenanes formed following fork rotation.

Consistent with the formation of excessive DNA pre-catenation destabilizing replication associated processes we observed a slight delay in anaphase onset in *tof1Δ* cells partially depleted of Top2 (Fig. 4B) and a pronounced G2/M delay following full depletion of Top2 in *tof1Δ* cells, (Fig. 4C, D). Cells deleted for *TOF1* or depleted of Top2 alone did not arrest in G2 (Fig. 4C, D) (14). This data suggests that a combination of *tof1Δ and* Top2 depletion, generates defects in the newly replicated chromatids that trigger cell cycle checkpoints.

Excessive fork rotation and DNA pre-catenation causes pre-mitotic DNA damage at yeast protein-DNA fragile sites

Deletion of Timeless causes constitutive DNA damage in human cells (25). Using H2A S129 phosphorylation (H2AS129P) as a marker for DNA damage we also

observed a significant increase in constitutive damage in *tof1Δ* cells in both S phase and post-replicative whole cell extracts (Fig. 5A). Depletion of Top2 alone led to less H2AS129P than in *tof1Δ*, but we observed the highest levels of H2AS129P in post-replicative cells with both *tof1Δ* and depleted Top2 (Fig. 5A). In these experiments the synchronized cultures were treated with nocodazole to avoid detection of damage generated during mitosis. Therefore the combination of excessive formation and stabilization of DNA pre-catenation during DNA replication appeared to lead to the highest levels of DNA damage in these cells. Consistent with this we also observed elevated activity of the DNA damage checkpoint effector kinase Rad53 in nocodazole arrested *tof1Δ top2-td* cells using the in-blot kinase assay (26), but not in similarly arrested *tof1Δ* or *top2* depleted cells (Fig. 5B). In addition, examination of post-replicative protein extracts also showed that PCNA mono-ubiquitylation was increased in *tof1Δ top2-td* cells (Fig. 5C) indicating that post-replication repair (PRR) was generally active following excessive fork rotation and DNA pre-catenation. This would be consistent with either gaps being left in the newly replicated sister chromatid, triggering PRR, or with ongoing PRR being inhibited by an abnormal sister chromatid structure. Together these data suggest that both excessive fork rotation and stabilization of pre-catenation lead to increased levels of constitutive DNA damage being detected on the newly replicated chromatids, with the combination of both sufficient to trigger widespread DNA repair and activation of the DNA damage checkpoint.

The apparent infliction of DNA damage within newly replicated chromatids following excessive DNA pre-catenation would predict that sites of constitutive fork rotation should be most affected by this pathway, potentially leading these sites to have elevated levels of DNA damage even in unchallenged wildtype cells. Others have identified all the yeast genomic loci that exhibit constitutively elevated levels of DNA

damage in wildtype yeast cells and have defined such sites as the yeast equivalent of mammalian fragile sites (27). Interestingly, this set includes tRNAs and inactive origins where elevated levels of DNA pre-catenation are likely to occur. In order to test if DNA damage detected at these fragile sites was linked to increased pre-catenation during DNA replication we examined how loss of Top2 and/or Tof1 altered H2A S129 phosphorylation at candidate fragile sites. ChIP analysis for H2AS129P demonstrated that the absence of Top2 and/or Tof1 during DNA replication led to significantly greater increases of DNA damage at two distinct genomic tRNA pausing sites compared to two tested euchromatic sites (Fig. 5D). Increased DNA damage was not due to passage through mitosis since these cells were arrested in nocodazole following passage through one S phase. We conclude that the elevated frequencies of fork rotation and DNA pre-catenation that occur at stable protein-DNA fragile sites is linked to DNA damage and fragile site instability.

Discussion

Previous studies of DNA pre-catenation have demonstrated the potential for fork rotation and pre-catenation to facilitate ongoing DNA replication in the face of topological stress *in vitro* (8-10). Here we show that this capability is actively restricted during DNA replication in budding yeast through the activity of the evolutionarily conserved Timeless/Tipin factors Tof1/Csm3. When this complex is present, fork rotation and pre-catenation is not determined by replicon size. Rather it appears that the presence of distinctive genomic features within the replicon alter how often fork rotation occurs during replication elongation. Outside of termination (6), we show that the presence of tRNA genes, inactive origins and possibly centromeres in plasmid replicons also increase the incidence of fork rotation during DNA replication. All these genomic contexts pause ongoing replication, presumably due to the stability of the protein-DNA complexes that they generate (16). We

speculate that these large stable complexes inhibit topoisomerase access to the underlying DNA, preventing relaxation of topological stress ahead of the fork, which results in fork rotation at these known hard to replicate and fragile loci (Fig. S8).

Our data suggests that the yeast replisome rarely rotates unless topoisomerase action ahead of the fork proves insufficient for ongoing replication. Potentially topoisomerase action could be similarly inhibited in other genomic contexts, for example at heterochromatin. Regions of transcriptionally induced overwinding, such as converging genes (28) or nuclear membrane attached genes (29), could also induce such high levels of topological stress that topoisomerase action ahead of the fork would be insufficient for ongoing replication. Therefore in all these contexts fork rotation could facilitate replication, resulting in local elevated DNA pre-catenation.

This restriction of fork rotation requires both Tof1 and Csm3, the yeast homologues of Timeless/Tipin. Deletion of *tof1/csm3* leads to diminished pausing at stable protein-DNA sites (19). Our data suggest that in wildtype cells Tof1/Csm3 inhibit fork rotation, and therefore DNA unwinding at such sites, contributing to pausing. In the absence of Tof1/Csm3 this inhibition is lifted leading to a more rapid transit of the pause site, utilizing fork rotation to unwind the DNA. Mechanistically, we speculate that Tof1/Csm3 could inhibit fork rotation in either of two ways. Loss of Timeless/Tipin orthologues disrupts replisome configuration (21, 22, 30). Potentially the mutant replisome could have a lower resistance to fork rotation than wildtype. Alternatively, Tof1 has been reported to interact with eukaryotic topoisomerase I (31). This interaction could maximize the local concentration of topoisomerase activity at the fork and minimize the need for fork rotation.

Whatever the exact mechanism of rotation inhibition, our data suggests that fork rotation and pre-catenation is minimized to prevent the generation of DNA damage in the newly replicated sister chromatids. Since yeast fragile sites accumulate both DNA catenation and DNA damage in pathways regulated by Tof1 and Top2 activity, our data argues that excessive fork rotation and DNA pre-catenation is closely linked with endogenous replicative damage and chromosome fragility. We hypothesize that this is through one of two pathways. First the incidence of fork rotation and DNA catenation could actually be a co-marker for other aberrant DNA transactions. High levels of topological stress ahead of a fork can lead to fork reversal (32) as well as fork rotation (9). Consistent with this possibility fork reversal is observed following trapping of Top1 complexes ahead of the fork (33). Potentially in a population of cells, both regression and rotation could be taking place within topologically stressed regions and inappropriate processing of reversed forks would lead to damage. Alternatively, high local levels of fork rotation and DNA pre-catenation could lead to braiding of the newly replicated sister chromatids (Fig. S8). Such braiding would inhibit several processes that occur in the immediate wake of the fork. Such processes include Okazaki fragment maturation, which would be consistent with the high levels of PCNA ubquitylation we observe (34), as well as intra-S checkpoint signaling and cohesion establishment. Since loss of Tof1/Timeless leads to gaps in the replicated chromosomes, loss of checkpoint signaling and mitotic cohesion defects (20) we currently favor this possibility. However, further investigation is required to determine the exact nature of the connection between fork rotation, DNA pre-catenation and fragile site instability.

Materials and Methods

Yeast Strains. Full genotypes are listed in *SI Appendix* Table S1.

Plasmids. Plasmids pRS426 and pRS316 described previously (13). To construct tRNApRS316, a fragment containing tA(AGC)F, tY(GUA)F1 and tF(GAA)F was produced by gene synthesis and SmaI cloned into pRS316. 7ARS-YIplac204 and 1ARS-YIplac204 were a gift from J. Diffley (35). To allow resolution on the same gel 1ARS-YIplac204 was extended by the AatII-EcoRI fragment of pRS316 (containing the *URA3* marker) cloned into AatII-MfeI. For larger plasmids, 3067bp BamHI/EcoRI fragment of pGT60 cloned into pRS316. additional 4400bp added by cloning NotI/SpeI fragment of mukB gene into 8kb plasmid.

Media and Cell Cycle Synchronisation. Spot test and alpha factor release experiments carried out as described (14). For *top2-4* strains, YPD (YP + 2% glucose) was used. Nocodozole at 10 µg/ml used where indicated.

Assessing plasmid DNA catenation. DNA was purified for resolution and non-radioactive Southern blotting and detection carried out as described (13). For catenation 2D gels the DNA was nicked with either Nb.BsmI or Nb.BsrDI (NEB), DNA first resolved in a 0.4% agarose (Megasieve, Flowgen) gel in 1x TBE at 1.2V/cm for 13-17h before being excised and embedded into a 0.8-1.2% (depending on plasmid size) agarose gel and resolved at 2-4.8V/cm in 1x TBE. Probes generated from pRS316 including *URA3*. Images were acquired by ImageQuant LAS4000 (GE Healthcare) and analysed using ImageQuant TL software.

Flow cytometry, western blotting, in-blot kinase assay and chromatin immuno-precipitation. Western blotting, Rad53 kinase assay carried out as described (14). Antibodies used anti-H2AP (Abcam, ab15083), anti-PGK1 antibody (Invitrogen, 459250), anti-PCNA antibody [5E6/2] (ab70472) (Abcam). Detection of PCNA ubiquitylation as described (34) and Chromatin immuno-precipitation carried out as described (36).

An extended description of all methods used in this study is provided in the *SI Appendix.*

Acknowledgments:

We thank members of G.D.S.C. for discussions and critical reading of the manuscript. This work was funded by the Royal Society (J. B.), by the Biotechnology and Biological Sciences Research Council United Kingdom (S.A.S.) and by Cancer Research U.K (A. L. C. and J. A. D.).

References

1. Brill SJ, DiNardo S, Sternglanz R (1987) Need for DNA topoisomerase activity as a swivel for DNA replication for transcription of ribosomal RNA. *Nature* 326(6111):414–416.

2. Bermejo R, et al. (2007) Top1- and Top2-mediated topological transitions at replication forks ensure fork progression and stability and prevent DNA damage checkpoint activation. *Genes & Development* 21(15):1921–1936.

3. Bermejo R, Lai MS, Foiani M (2012) Preventing replication stress to maintain genome stability: resolving conflicts between replication and transcription. *Molecular Cell* 45(6):710–718.

4. Champoux JJ, Been MD (1980) *TOPOISOMERASES AND THE SWIVEL PROBLEM* (ACADEMIC PRESS, INC.).

5. Baxter J (2015) “Breaking up is hard to do”: the formation and resolution of sister chromatid intertwines. *Journal of Molecular Biology* 427(3):590–607.

6. Sundin O, Varshavsky A (1980) Terminal stages of SV40 DNA replication proceed via multiply intertwined catenated dimers. *Cell* 21(1):103–114.

7. Sundin O, Varshavsky A (1981) Arrest of segregation leads to accumulation of highly intertwined catenated dimers: dissection of the final stages of SV40 DNA replication. *Cell* 25(3):659–669.

8. Hiasa H, Marians KJ (1994) Topoisomerase III, but not topoisomerase I, can support nascent chain elongation during theta-type DNA replication. *J Biol Chem* 269(51):32655–32659.

9. Peter BJ, Ullsperger C, Hiasa H, Marians KJ, Cozzarelli NR (1998) The structure of supercoiled intermediates in DNA replication. *Cell* 94(6):819–827.

10. Lucas I, Germe T, Chevrier-Miller M, Hyrien O (2001) Topoisomerase II can

unlink replicating DNA by precatenane removal. *The EMBO Journal* 20(22):6509–6519.

11. Postow L, Hardy CD, Crisona NJ, Peter BJ, Cozzarelli NR (2001) Topological challenges to DNA replication: conformations at the fork. *Proc Natl Acad Sci USA* 98(15):8219–8226.

12. Martinez-Robles ML, et al. (2009) Interplay of DNA supercoiling and catenation during the segregation of sister duplexes. *Nucleic Acids Research* 37(15):5126–5137.

13. Baxter J, et al. (2011) Positive Supercoiling of Mitotic DNA Drives Decatenation by Topoisomerase II in Eukaryotes. *Science* 331(6022):1328–1332.

14. Baxter J, Diffley JF (2008) Topoisomerase II inactivation prevents the completion of DNA replication in budding yeast. *Molecular Cell* 30(6):790–802.

15. Holm C, Goto T, Wang JC, Botstein D (1985) DNA topoisomerase II is required at the time of mitosis in yeast. *Cell* 41(2):553–563.

16. Ivessa AS, et al. (2003) The Saccharomyces cerevisiae helicase Rrm3p facilitates replication past nonhistone protein-DNA complexes. *Molecular Cell* 12(6):1525–1536.

17. Hogan E, Koshland DE (1992) Addition of extra origins of replication to a minichromosome suppresses its mitotic loss in cdc6 and cdc14 mutants of Saccharomyces cerevisiae. *Proceedings of the National Academy of Sciences* 89(7):3098–3102.

18. Brewer BJ, Fangman WL (1994) Initiation preference at a yeast origin of replication. *Proc Natl Acad Sci USA* 91(8):3418–3422.

19. Hodgson B, Calzada A, Labib K (2007) Mrc1 and Tof1 Regulate DNA Replication Forks in Different Ways during Normal S Phase. *Molecular Biology of the Cell* 18(10):3894–3902.

20. Leman AR, Noguchi E (2012) Local and global functions of Timeless and Tipin in replication fork protection. *cc* 11(21):3945–3955.

21. Katou Y, et al. (2003) S-phase checkpoint proteins Tof1 and Mrc1 form a stable replication-pausing complex. *Nature* 424(6952):1078–1083.

22. Errico A, et al. (2009) Tipin/Tim1/And1 protein complex promotes Pol alpha; chromatin binding and sister chromatid cohesion. *The EMBO Journal* 28(23):3681–3692.

23. Tourriere H, Versini G, Cordón-Preciado V, Alabert C, Pasero P (2005) Mrc1 and Tof1 Promote Replication Fork Progression and Recovery Independently of Rad53. *Molecular Cell* 19(5):699–706.

24. Putnam CD, Hayes TK, Kolodner RD (2009) Specific pathways prevent duplication- mediated genome rearrangements. *Nature* 460(7258):984–989.

25. Chou DM, Elledge SJ (2006) Tipin and Timeless form a mutually protective complex required for genotoxic stress resistance and checkpoint function. *Proc Natl Acad Sci USA* 103(48):18143–18147.

26. Pellicioli A, et al. (1999) Activation of Rad53 kinase in response to DNA damage and its effect in modulating phosphorylation of the lagging strand DNA polymerase. *The EMBO Journal* 18(22):6561–6572.

27. Szilard RK, et al. (2010) Systematic identification of fragile sites via genome-wide location analysis of gamma-H2AX. *Nat Struct Mol Biol* 17(3):299–305.

28. Jeppsson K, et al. (2014) The chromosomal association of the Smc5/6 complex depends on cohesion and predicts the level of sister chromatid entanglement. *PLoS Genet* 10(10):e1004680.

29. Bermejo R, et al. (2011) The replication checkpoint protects fork stability by releasing transcribed genes from nuclear pores. *Cell* 146(2):233–246.

30. Cho W-H, et al. (2013) Human Tim-Tipin complex affects the biochemical properties of the replicative DNA helicase and DNA polymerases. *Proc Natl Acad Sci USA* 110(7):2523–2527.

31. Park H, Sternglanz R (1999) Identification and characterization of the genes for two topoisomerase I-interacting proteins from Saccharomyces cerevisiae. *Yeast* 15(1):35–41.

32. Postow L, et al. (2001) Positive torsional strain causes the formation of a four-way junction at replication forks. *J Biol Chem* 276(4):2790–2796.

33. Chaudhuri AR, et al. (2012) Topoisomerase I: poisoning results in PARP-mediated replication fork reversal. *Nature Genetics* 19(4):417–423.

34. Karras GI, Jentsch S (2010) The RAD6 DNA Damage Tolerance Pathway Operates Uncoupled from the Replication Fork and Is Functional Beyond S Phase. *Cell* 141(2):255–267.

35. Tanaka S, Diffley JF (2002) Deregulated G1-cyclin expression induces genomic instability by preventing efficient pre-RC formation. *Genes & Development* 16(20):2639–2649.

36. Chambers AL, et al. (2012) The INO80 chromatin remodeling complex prevents polyploidy and maintains normal chromatin structure at centromeres. *Genes & Development* 26(23):2590–2603.

Figure Legends

Figure 1

Fork rotation and DNA catenation occurs on replication through stable protein-DNA pause sites.

(A-C and E-H) Cells containing the *top2-4* allele and plasmid (A) pR316 (B) pRS316 containing 3kb (C) or 7kb of additional bacterial sequence, (E) pRS426, (F) CEN and 3x tRNA genes plasmid tRNApRS316, (G) YIPlac plasmid with 1xARSH4 or (H) 7xARSH4 origins in a YIPlac plasmid (represented in cartoon format) were assessed for DNA catenation following one round of DNA replication in the absence of Top2 activity (representative autoradiograms shown). Histograms showing the relative intensity of catenanes containing 1 to 27 catenanes are shown, along with median of the whole distribution and % of catenanes from plasmids with >20 catenanes. Arrows indicate mobility of plasmids containing 1 catenane (CatAn=1) and 20 (CatAn=20). Histograms and % of plasmids > 20 catenanes represent the average of ≥ 3 independent experiments. Error bars or values are average deviation. See Fig.S2 for full explanation.

(C) Model for topoisomerase exclusion at both termination (left) and stable protein-DNA structures (right). As replisomes converge, topoisomerases are sterically inhibited from relaxing helical tension in the final few turns. Therefore fork rotation is required for unwinding. Theoretically a similar situation arises when a replisome approaches a stable protein-DNA complex.

Figure 2

The yeast *Timeless* and *Tipin* homologues *TOF1* and *CSM3* and the displacement helicase *RRM3* are required to restrict fork rotation and DNA catenation.

DNA catenation analysis of plasmid pRS316 in *top2-4* cells and the different deletion alleles (A) *tof1Δ*, (B) *csm3Δ*, (C) *mrc1Δ,* (D) *rrm3Δ* were analyzed as in Fig. 1. Histograms and % of plasmids > 20 or >30 catenanes represent the average of ≥ 2 independent experiments. See *SI Appendix* Fig. S2 for full explanation.

Figure 3

Rrm3 limits the frequency of fork rotation and pre-catenation at stable protein-DNA isites while Tof1 acts more generally.

Cells deleted for *RRM3* and containing the *top2-4* allele and (A) plasmid pRS426 or (B) plasmid tRNApRS316 and cells deleted for *TOF1* and containing the *top2-4* allele and (C) plasmid pRS426, or (D) plasmid tRNApRS316 were cultured, collected, DNA prepared and DNA catenation analysis carried out as described in Fig. 1.

Figure 4

Deletion of *TOF1* triggers excessive catenation of endogenous chromosomes and G2 cell cycle arrest.

(A) Viability assay of strains under the permissive condition of growth on YPD at 25°C or with partial transcriptional repression of TOP2 (+doxycycline). (B) Deletion of *TOF1* causes chromosome non-disjunction following partial depletion of Top2 activity. Cells grown under semi-restrictive conditions following synchronous release from G1 and analysed for chromosome mis-segregation by FACs for DNA content (left panel) or cytological analysis for “cut” and divided nuclei. Examples of “cut” cells (arrow heads) shown (right) (DAPI stained DNA (blue) shown over light image of cells).

(C) Indicated strains arrested in alpha factor and Top2 degraded (YPRaf Gal, 37°C +doxycycline). Samples were taken at mid-log phase (25°C exp), prior to alpha factor release (0) and at time points shown for analysis FACS to assess DNA content (left) or nuclear cytologies of cells (right). % of single (diamonds and solid line) or divided nuclei (squares and dashed line) shown.

Figure 5

Unrestricted fork rotation and excessive DNA catenation causes DNA damage and extended post-replicative repair of replicated chromatids.

(A) Indicated cells released from alpha factor following Top2 depletion, into a nocodazole arrest. Samples from timepoints analyzed by western blot for phosphorylation of H2A S129 (PGK1 used for loading control) and FACS for DNA.

(B) Experiment carried out as in (A) but samples were assayed for Rad53 activation using the Rad53 auto-phosphorylation assay. Control samples of MMS treated exponential *top2-td and rad53*Δ *top2-td* cells also shown.

(C) PCNA ubiquitylation monitored in post-replicative cells (80 min following release) by western blotting. Blotting for PCNA in MMS treated cells containing either HIS-tagged wild type PCNA or HIS-tagged K164R confirmed specificity of PCNA antibody for mono-ubiquitylated PCNA (U1) or poly-ubiquitylated PCNA (U2).

(D) Chromatin immunoprecipitation (ChIP) of H2A S129 phosphorylation at tRNA, and euchromatic loci in isogenic *top2-td, tof1*Δ, and *tof1*Δ *top2-td* strains following one S phase under the restrictive conditions relative to wildtype cells. ChIP signal was normalized to amplification of input DNA prior to calculation of the relative change at each locus in wildtype cells. Data shown are the mean of three independent experiments +/-1 SD.

Schalbetter_Fig1

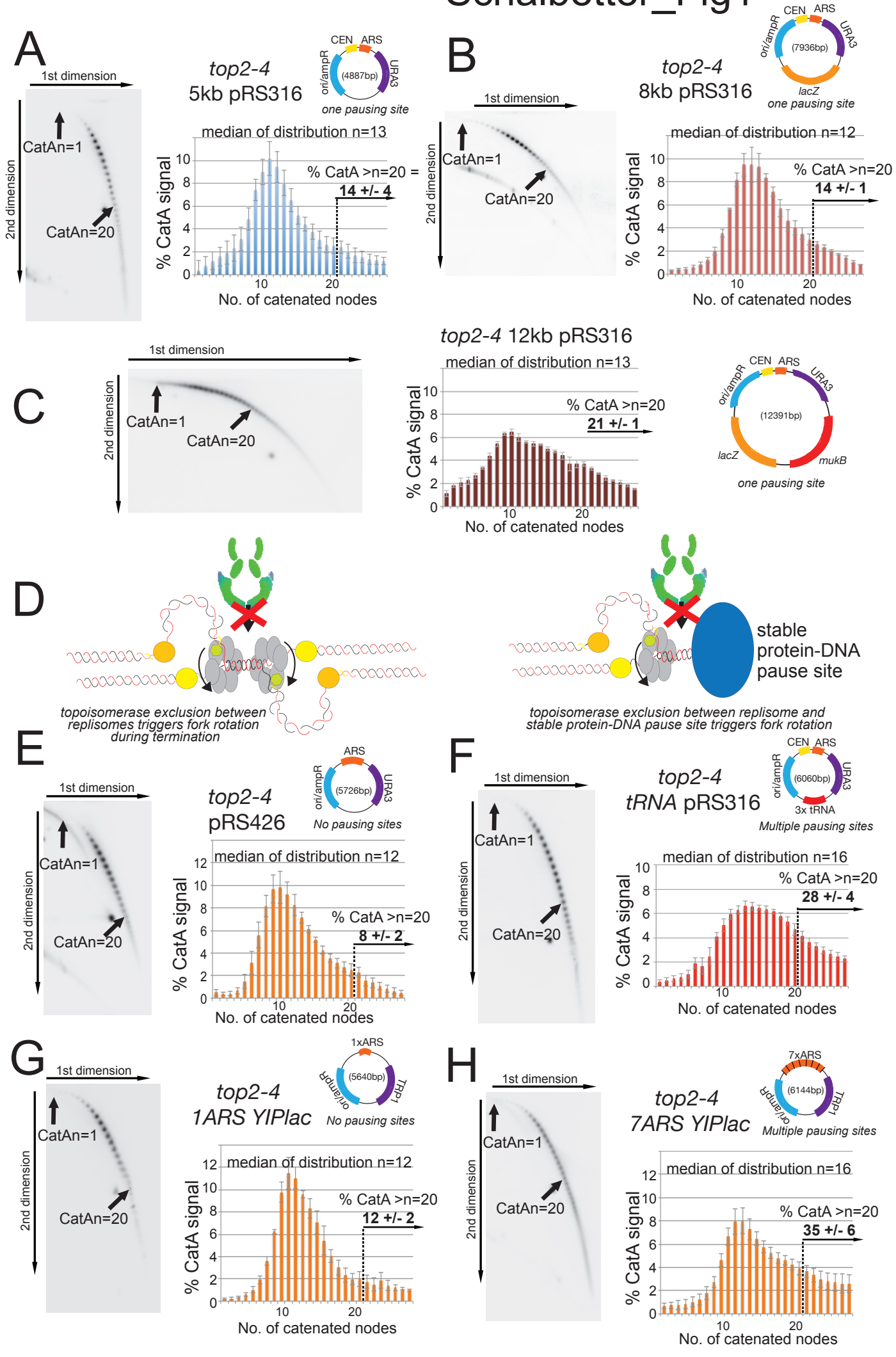

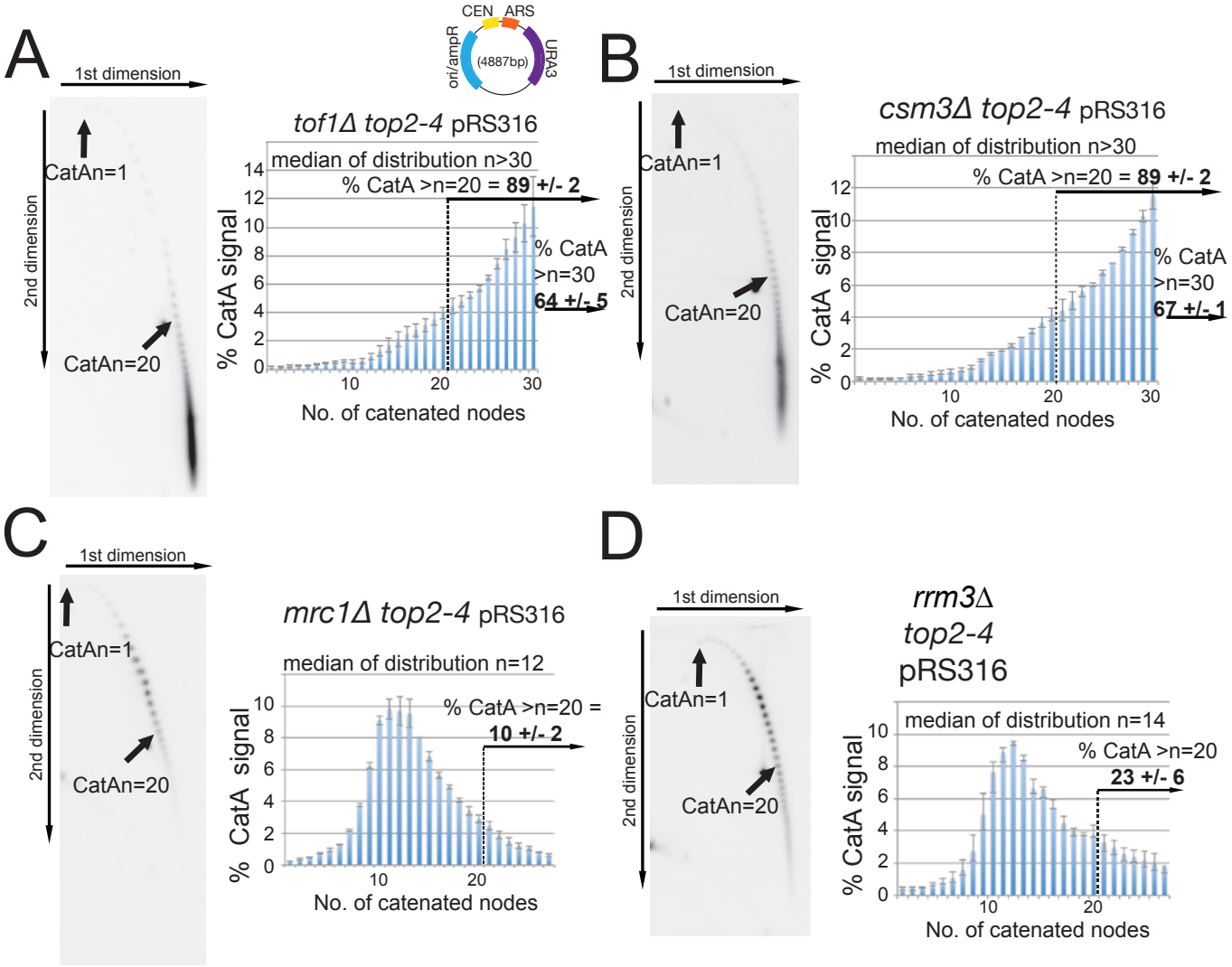
A
1st dimension
2nd dimension
CatAn=1
CatAn=20
CEN
ARS
ori/ampR
URA3
(4887bp)
tof1Δ top2-4 pRS316
median of distribution n>30
% CatA >n=20 = 89 +/- 2
% CatA >n=30 64 +/- 5
% CatA signal
No. of catenated nodes
B
1st dimension
2nd dimension
CatAn=1
CatAn=20
csm3Δ top2-4 pRS316
median of distribution n>30
% CatA >n=20 = 89 +/- 2
% CatA >n=30 67 +/- 1
% CatA signal
No. of catenated nodes
C
1st dimension
2nd dimension
CatAn=1
CatAn=20
mrc1Δ top2-4 pRS316
median of distribution n=12
% CatA >n=20 = 10 +/- 2
% CatA signal
No. of catenated nodes
D
1st dimension
2nd dimension
CatAn=1
CatAn=20
rrm3Δ top2-4 pRS316
median of distribution n=14
% CatA >n=20 23 +/- 6
% CatA signal
No. of catenated nodes

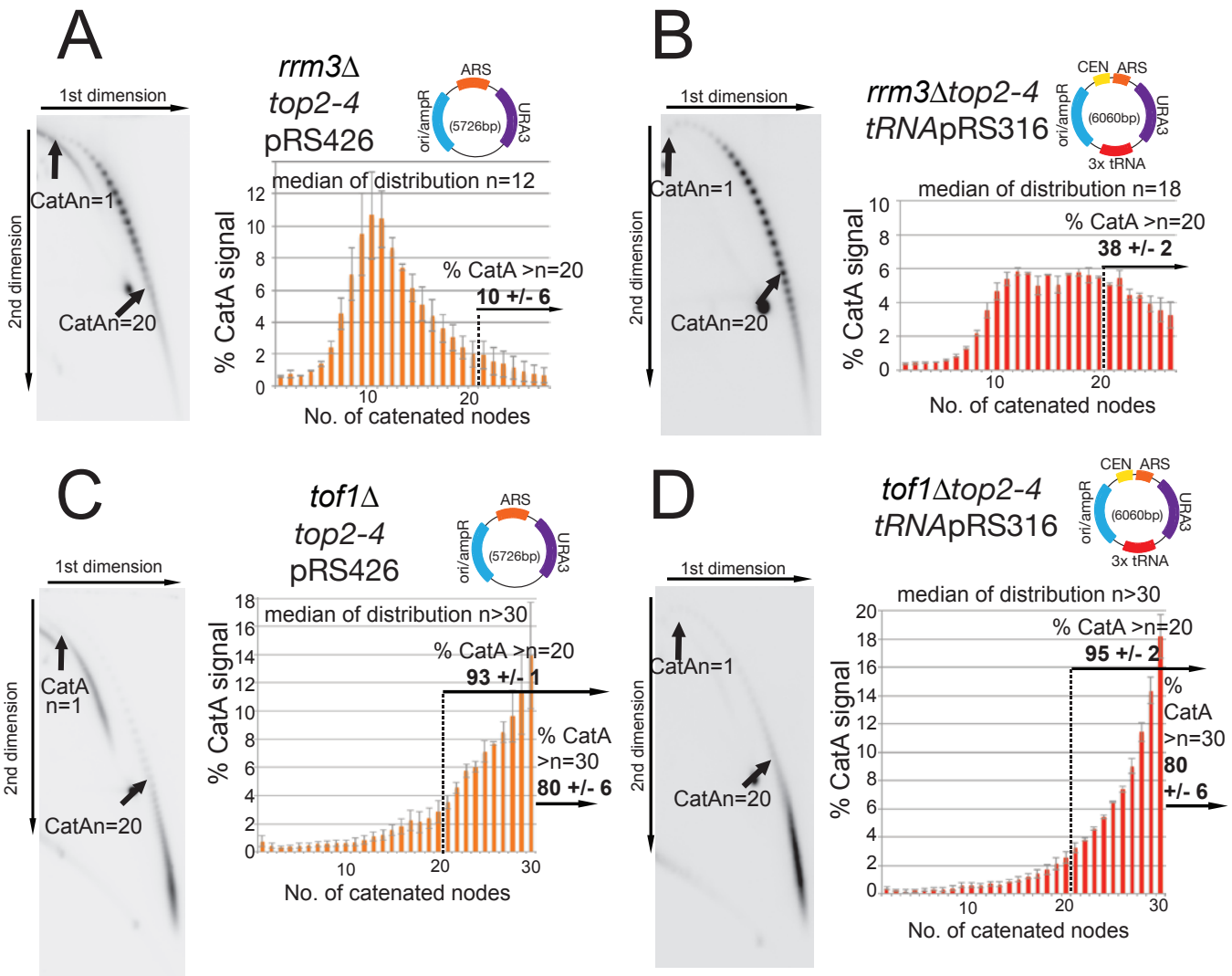
A
1st dimension
2nd dimension
CatAn=1
CatAn=20
rrm3Δ
top2-4
pRS426
ARS
ori/ampR
URA3
(5726bp)
median of distribution n=12
% CatA >n=20
10 +/- 6
% CatA signal
No. of catenated nodes
B
1st dimension
2nd dimension
CatAn=1
CatAn=20
rrm3Δtop2-4
tRNApRS316
CEN ARS
ori/ampR
URA3
(6060bp)
3x tRNA
median of distribution n=18
% CatA >n=20
38 +/- 2
% CatA signal
No. of catenated nodes
C
1st dimension
2nd dimension
CatA
n=1
CatAn=20
tof1Δ
top2-4
pRS426
ARS
ori/ampR
URA3
(5726bp)
median of distribution n>30
% CatA >n=20
93 +/- 1
% CatA
>n=30
80 +/- 6
% CatA signal
No. of catenated nodes
D
1st dimension
2nd dimension
CatAn=1
CatAn=20
tof1Δtop2-4
tRNApRS316
CEN ARS
ori/ampR
URA3
(6060bp)
3x tRNA
median of distribution n>30
% CatA >n=20
95 +/- 2
% CatA
>n=30
80
+/- 6
% CatA signal
No. of catenated nodes

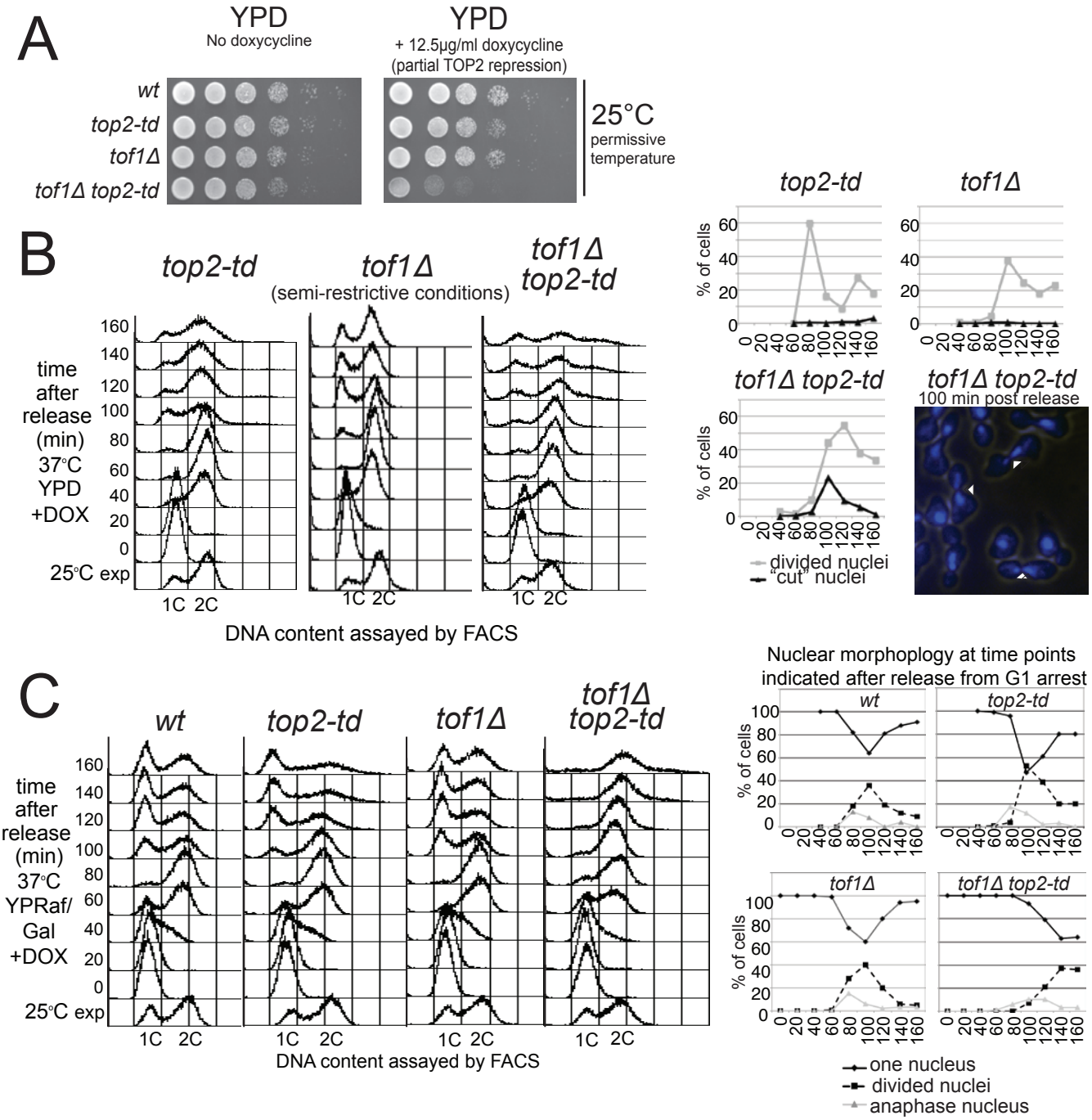
A
YPD
No doxycycline
YPD
+ 12.5µg/ml doxycycline
(partial TOP2 repression)
wt
top2-td
tof1Δ
tof1Δ top2-td
25°C
permissive
temperature
B
top2-td
tof1Δ
(semi-restrictive conditions)
tof1Δ
top2-td
time
after
release
(min)
37°C
YPD
+DOX
25°C exp
1C 2C
DNA content assayed by FACS
top2-td
tof1Δ
% of cells
tof1Δ top2-td
tof1Δ top2-td
100 min post release
divided nuclei
"cut" nuclei
C
wt
top2-td
tof1Δ
tof1Δ
top2-td
time
after
release
(min)
37°C
YPRaf/
Gal
+DOX
25°C exp
1C 2C
DNA content assayed by FACS
Nuclear morphology at time points
indicated after release from G1 arrest
wt
top2-td
tof1Δ
tof1Δ top2-td
% of cells
one nucleus
divided nuclei
anaphase nucleus

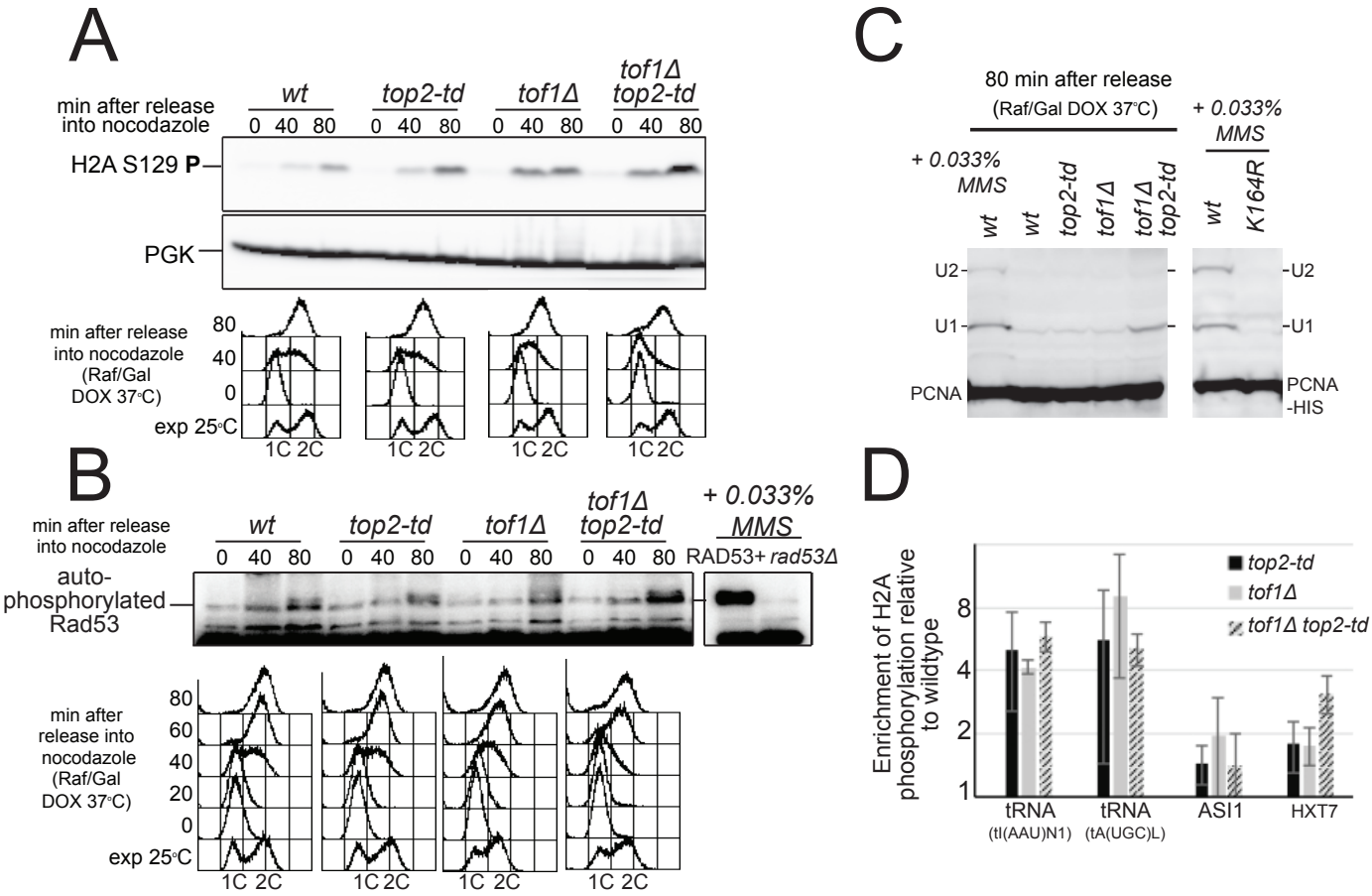
A
min after release into nocodazole
wt
top2-td
tof1Δ
tof1Δ top2-td
0 40 80 0 40 80 0 40 80 0 40 80
H2A S129 P
PGK
min after release into nocodazole (Raf/Gal DOX 37°C)
80
40
0
exp 25°C
1C 2C
B
min after release into nocodazole
wt
top2-td
tof1Δ
tof1Δ top2-td
+ 0.033% MMS
0 40 80 0 40 80 0 40 80 0 40 80
RAD53+ rad53Δ
auto-phosphorylated Rad53
min after release into nocodazole (Raf/Gal DOX 37°C)
80
60
40
20
0
exp 25°C
1C 2C
C
80 min after release
(Raf/Gal DOX 37°C)
+ 0.033% MMS
+ 0.033% MMS
wt
wt
top2-td
tof1Δ
tof1Δ top2-td
wt
K164R
U2
U1
PCNA
U2
U1
PCNA -HIS
D
Enrichment of H2A phosphorylation relative to wildtype
top2-td
tof1Δ
tof1Δ top2-td
8
4
2
1
tRNA (tI(AAU)N1)
tRNA (tA(UGC)L)
ASI1
HXT7

Fork rotation and DNA pre-catenation is restricted during DNA replication to prevent chromosomal instability

S. A. Schalbetter, S. Mansoubi, A. L. Chambers, J. A. Downs and J. Baxter

SI Appendix

Contents

Supplemental Material and Methods	p2
SI Appendix Figure Legends	p5
Table S1 - Yeast strains	p9
Table S2 – Summary of DNA catenation assays	p10
SI Appendix Figures	p11

Supplemental Material and Methods:

Methods

Yeast Strains

Yeast containing *top2-td* were derived from W303-1a (*MATa ade2-1 ura3-1 his3-11, trp1-1 leu2-3, can1-100*), *top2-4* cells derived from (Holm et al. 1985). Full genotypes are listed in Table S1.

Media and Cell Cycle Synchronisation

Top2-td cell cultures for alpha factor release experiments were prepared as described previously (Baxter and Diffley 2008). For plasmid experiments with *top2-4* strains, yeast cells were grown in minimal media 2% glucose selecting for the plasmid (-ura or -trp) to log phase at 25°C before transferring to YP +ade 2% glucose and grown to midlog phase. Cells were then arrested in G1 with 10μg/ml alpha factor until 90% of cells were in G1 (120 min). The culture was incubated at 37°C for 1h and cells were released from the block into YP +ade 2% Glucose. Time 0 was taken as time of addition of first wash. Nocodozole was added to cultures at 10 μg/ml. Samples were taken at the indicated time points, pelleted and frozen on dry ice.

Flow cytometry (FACS) analysis

For FACS analysis cells were prepared as described previously {Baxter:2008hn}.

DNA preparation

DNA was extracted as described in Baxter et al. 2011 (Baxter et al. 2011).

Gel electrophoresis for detection of plasmid catenation

For catenation 2D gels the DNA was nicked with either Nb.BsmI or Nb.BsrDI (NEB) according to the manufacturer's instructions.

Nicked catenanes were separated in the first dimension on a 0.4% agarose (Megasieve, Flowgen) gel in 1x TBE at 1.2V/cm for 13-17h at room temperature. The respective lanes were excised and embedded into a 0.8-1.2% (depending on plasmid size) agarose (Megasieve, Flowgen) gel and run at 2-4.8V/cm in 1x TBE (in the coldroom if more than 2V/cm were used). Non-radioactive Southern blotting and detection were carried out as described (Baxter et al. 2011). Blots were probed with either DNA amplified from sequences of pRS316 including the URA3 sequences or from pRS314 including the TRP1 gene as appropriate. Non-saturating exposures of the blot were acquired by an ImageQuant LAS4000 (GE Healthcare) and densitometry analysis carried out using ImageQuant TL software. Overexposed images were taken to clearly identify the CatAn=1 signal, which was often weak in non-saturating exposures.

Protein Extraction and analysis

Whole protein extracts were prepared by alkaline lysis followed by TCA precipitation. Cells were resuspended in lysis buffer (1.85M NaOH, 7.5% β-Mercaptoethanol) and incubated on ice for 15min. Proteins were precipitated with TCA (6.4% final concentration) on ice for 10min. Precipitates were resuspended in HU buffer (8M urea, 5% SDS, 200mM Tris-HCl pH6.8, 1mM EDTA, 1.5% DTT, bromophenol blue) and separated by 15% SDS-PAGE. Phosphorylation of S129 of H2A and PGK1 expression have been detected using antibody against H2Ap (Abcam, ab15083) and anti-PGK1 antibody (Invitrogen, 459250). Detection of PCNA ubiquitylation as described in Karras and Jentsch {Karras:2010kj} using anti-PCNA antibody [5E6/2] (ab70472) (Abcam).

Rad53 Kinase assay

In situ autophosphorylation assay was carried out as described {Pellicioli:1999bn}.

Chromatin Immunoprecipitation of H2A S129 Phosphorylation.

Synchronized cultures were fixed with 1% formaldehyde for 10 min at room temperature before immunoprecipitation with anti-phospho H2A S129 antibody (Abcam ab15083). CHIP assays were performed essentially as in {StrahlBolsinger:1997vv}. Immunoprecipitated and input DNA was quantified by qPCR. Enrichment was analyzed at at tRNA loci tI(AAU)N1 and tA(UGC)L, and within the euchromatic loci *ASI1* and *HXT7* (primer sequences available on request). ChIP signal was normalized to amplification from input DNA and expressed relative to wt. Data shown is the mean enrichment +/- 1SD.

SI Appendix Figure Legends

Figure S1

Model of topological stress generation and relaxation during elongation of DNA replication. (A) During elongation, unwinding of the parental template separates the parental strands but does not resolve the linkages that exist between the two strands. (B) The linkages between the strands are displaced into the region ahead of the fork leading to this becoming overwound, i.e. positively supercoiled (+). (C) This tension is normally resolved by the action of either topoisomerase I (Top1) or topoisomerase II (Top2), which act as effective “swivelases” ahead of the fork to generate a (D) relaxed replication region. (E) However, Champoux and Been proposed a second mode of topological stress unwinding where the helical tension is relaxed by rotation of the fork to generate DNA pre-catenation behind the fork. Although these linkages should not arrest forward elongation of replication, it is essential that the type II topoisomerase II (Top2) resolves all DNA catenation before the completion of cell division.

Figure S2

Quantification of fork rotation during DNA replication. In wildtype cells Top2 decatenates both pre-catenanes and catenanes formed during DNA replication. Therefore to assay how often fork rotation and pre-catenation occurs during replication on a plasmid replicon we allow one round of replication in the absence of Top2 activity and collect DNA from the cells blocked in G2 by nocodazole, 80 minutes after release into the cell cycle (plasmid products shown in left hand panel). The catenated products of replication in this background are negatively supercoiled due to nucleosome deposition in the sister chromatids. Supercoiling in de-proteinized plasmids normally compacts all catenated states into an unresolvable

population. In order to resolve individual catenated states the purified DNA is treated with a site-specific nicking enzyme to remove supercoiling but maintain catenated nodes. The nicked DNA is resolved by agarose gel electrophoresis on two separate dimensions to be able to resolve both low and high catenated states before Southern blotting and probing for plasmid sequences (middle panel). The relative intensities of each state were then calculated by densitometry in two ways. First by quantifying signal in equally sized regions centred on each catenated signal state on states 1 to 27 (or 1-30 for hypercatenated samples where the signal >27 were definable), correcting for local background and then expressing the relative intensity as a % of the total signal in all regions. The second measure was to compare the signal from the arc related to states 1 to 20 to states 21 and above. For this measure regions were drawn around all states 1 to 20 and from the remainder of the arc of relating to 21 and above. Then each set of states is expressed as a % of the sum of both. This measure has the advantage of being able to quantify the signal from the individually unresolvable catenated states that produced detectable signal.

Figure S3

Quantification of DNA catenation is directly related to incidence of fork rotation on plasmids.

(A) Deletion of TOP3 does not alter the level of DNA catenation generated in catenated plasmids. DNA catenation analysis of plasmid pRS316 in *sgs1Δ top3Δ top2-4* cells were analyzed as in Fig. 1. Histograms and % of plasmids > 20 catenanes represent the average of 2 independent experiments. Error bars or values are equal to the average deviation of the experiments.

(B) No residual decatenation activity can be detected in *top2-4* cells maintained under the restrictive conditions. DNA catenation analysis of plasmid pRS316 in

top2-4 cells isolated either 50 minutes or 110 minutes after release from alpha factor arrest. DNA was analysed as described in Fig.1

Figure S4

Deletion of CTF4 does significantly increase DNA catenation in pRS316

DNA catenation analysis of plasmid pRS316 in *ctf4Δ top2-4* cells, analyzed as in Fig. 1. Histograms and % of plasmids > 20 represent the average of 2 independent experiments. Error bars or values are equal to the average deviation of the experiments.

Figure S5

Model for how Rrm3 displacement activity alters fork rotation at stable protein-DNA fragile sites.

As the replisome approaches a stable protein-DNA complex, topoisomerases are inhibited from acting between the complex and the converging replisome. (A) If the Rrm3 helicase is active at the site, the protein complex will be rapidly displaced, allowing access of topoisomerases ahead of the fork and the curtailing of replisome rotation and DNA catenation. (B) If *RRM3* is deleted then rotation continues until the replisome itself physically displaces the stable protein complex, thereby allowing access for topoisomerases ahead of the fork. However, in this case more rotation-coupled unwinding is required until the protein complex is displaced.

Figure S6

Artificial slowing of replication elongation does not increase fork rotation and DNA catenation. (A) DNA catenation analysis of plasmid pRS316 in *top2-4* cells released from alpha factor arrest into 200mM hydroxyurea. The cells were collected 80 minutes after release and extracted DNA analysed as described in Fig.1. (B) DNA catenation analysis of plasmid pRS316 in *dpb3Δ top2-4* cells. (C) FACS analysis of *dpb3Δ* and *dpb3Δ top2-td* cells following release from alpha factor in the restrictive

condition shown that deletion *DPB3* appears to significantly slow down S phase, consistent with its known role as a polymerase epsilon processivity factor.

Figure S7

Western blot analysis of Top2 in exponential cells, grown under the semi-restrictive conditions in *wt*, *top2-td* and *tof1Δ top2-td* cells. PGK1 western blot of the same lanes is shown for loading comparison.

Figure S8

Viability assay of wildtype (wt), *top2-td*, *tof1Δ*, *tof1Δ top2-td, mrc1Δ* and *mrc1Δ top2-td* cells under the permissive condition of growth on YPD at 25°C or conditions of partial transcriptional repression of TOP2 (+doxycycline). (B) Partial depletion of Top2 activity does not lead to an increase in "cut" mitosis in *mrc1Δ* cells. *top2-td, mrc1Δ* and *mrc1Δ top2-td* cells grown under semi-restrictive conditions (YPD, 37°C +doxycycline) following synchronous release from G1 were analysed for cytological analysis for "cut" and divided nuclei and chromosomal aneuploidy by cellular DNA content using FACS analysis (bottom).

Figure S9

Model of causes and consequences of fork rotation and pre-catenation. During normal DNA replication the Tof1/Csm3 structured replisome inhibts to fork rotation and topoisomerases act ahead of the fork (left column). At certain genomic contexts, such as stable-protein-DNA structures topoisomerase are impeded from acting ahead of the fork (right, top). Here fork rotation aids unwinding resulting in elevated pre-catenation. Excessive pre-catenation could impede several processes including Okazaki fragment maturation resulting in gaps in the newly replicated chromosomes that require repair and leave chromatids fragile.

Table S1 – Yeast strains

top2-4	top2-4 Mat a his4-539 lys2-801 ura3-52[18]
top2-4 pRS316	top2-4 pRS316 Mat a his4-539 lys2-801 ura3-52
top2-4 pRS426	top2-4 pRS426 Mat a his4-539 lys2-801 ura3-52
top2-4 tRNA-pRS316	top2-4 tRNA-pRS316 Mat a his4-539 lys2-801 ura3-52
*top2-4 tof1*Δ pRS316	top2-4 3tRNA-pRS316 Mat a his4-539 lys2-801 ura3-52 tof1::hphMX
*top2-4 tof1*Δ pRS426	top2-4 pRS426 Mat a his4-539 lys2-801 ura3-52 tof1::hphMX
*top2-4 tof1*Δ tRNApRS316	top2-4 tRNA-pRS316 Mat a his4-539 lys2-801 ura3-52 tof1::hphMX
*top2-4 csm3*Δ pRS316	top2-4 pRS316 Mat a his4-539 lys2-801 ura3-52 csm3::natMX
*top2-4 mrc1*Δ pRS316	top2-4 pRS316 Mat a his4-539 lys2-801 ura3-52 mrc1::natMX
*top2-4 ctf4*Δ pRS316	top2-4 pRS316 Mat a his4-539 lys2-801 ura3-52 ctf4::natMX
*top2-4 sgs1*Δ *top3*Δ pRS316	top2-4 pRS316 Mat a his4-539 lys2-801 ura3-52 sgs1::NATNT2 top3::hphMX
*top2-4 dpb3*Δ pRS316	top2-4 pRS316 Mat a his4-539 lys2-801 ura3-52 dpb3::natMX
yST114 (wt)	MATa ade2-1 ura3-1 his3-11, trp1-1, can1-100 UBR1::pGAL-myc-UBR1 (HIS3), leu2-3 LEU2::pCM244 x3
top2-td	yST114 + kanMX-tTA-tetO2-UB-DHFRts-myc-top2
*top2-td tof1*Δ	yST114 + kanMX-tTA-tetO2-UB-DHFRts-myc-top2 tof1::hphMX
*top2-td dpb3*Δ	yST114 + kanMX-tTA-tetO2-UB-DHFRts-myc-top2 dpb3::natNT2
*dpb3*Δ	yST114 + dpb3::natNT2
*top2-td mrc1*Δ	top2-td + mrc1::hphMX
*mrc1*Δ	yST114 + mrc1::hphMX
*tof1*Δ	yST114 + tof1::hphMX

Table S2 – Summary of DNA catenation quantification experiments

Strain	Plasmid size (bp)	Number of replicates	Median CatAn=	% >20
top2-4 pRS316	4887	5	**13**	**14** +/-4
top2-4 8kb pRS316	7936	3	**12**	**14** +/-1
top2-4 12kb pRS316	12391	3	**13**	**21** +/-1
top2-4 pR426	5726	5	**12**	**8** +/-2
top2-4 tRNApRS316	6060	7	**16**	**28** +/-4
top2-4 1ori YIPlac	5640	4	**12**	**12** +/-2
top2-4 7ori YIPlac	6144	5	**16**	**35** +/-6
tof1Δ top2-4 pRS316	4887	2	**>30**	**89** +/-2
tof1Δ top2-4 pRS426	5726	2	**>30**	**93** +/-1
tof1Δ top2-4 tRNApRS316	6060	2	**>30**	**95** +/-2
csm3Δ top2-4 pRS316	4887	2	**>30**	**89** +/-2
mrc1Δ top2-4 pRS316	4887	2	**12**	**10** +/-2
ctf4Δ top2-4 pRS316	4887	2	**12**	**17** +/-7
rrm3Δ top2-4 pRS316	4887	2	**14**	**23** +/-6
rrm3Δ top2-4 pRS426	5726	2	**12**	**10** +/-6
rrm3Δ top2-4 tRNApRS316	6060	2	**18**	**38** +/-2
sgs1Δ top3Δ top2-4 pRS316	4887	2	**12**	**17** +/-1
top2-4 pRS316 + 200mM HU	4887	2	**11**	**11** +/-1

Median calculated as explained in Fig. S2

Schalbetter_ Fig. S1

Supplemental information for Introduction;
Topological stress generation and relaxation
during elongation of DNA replication

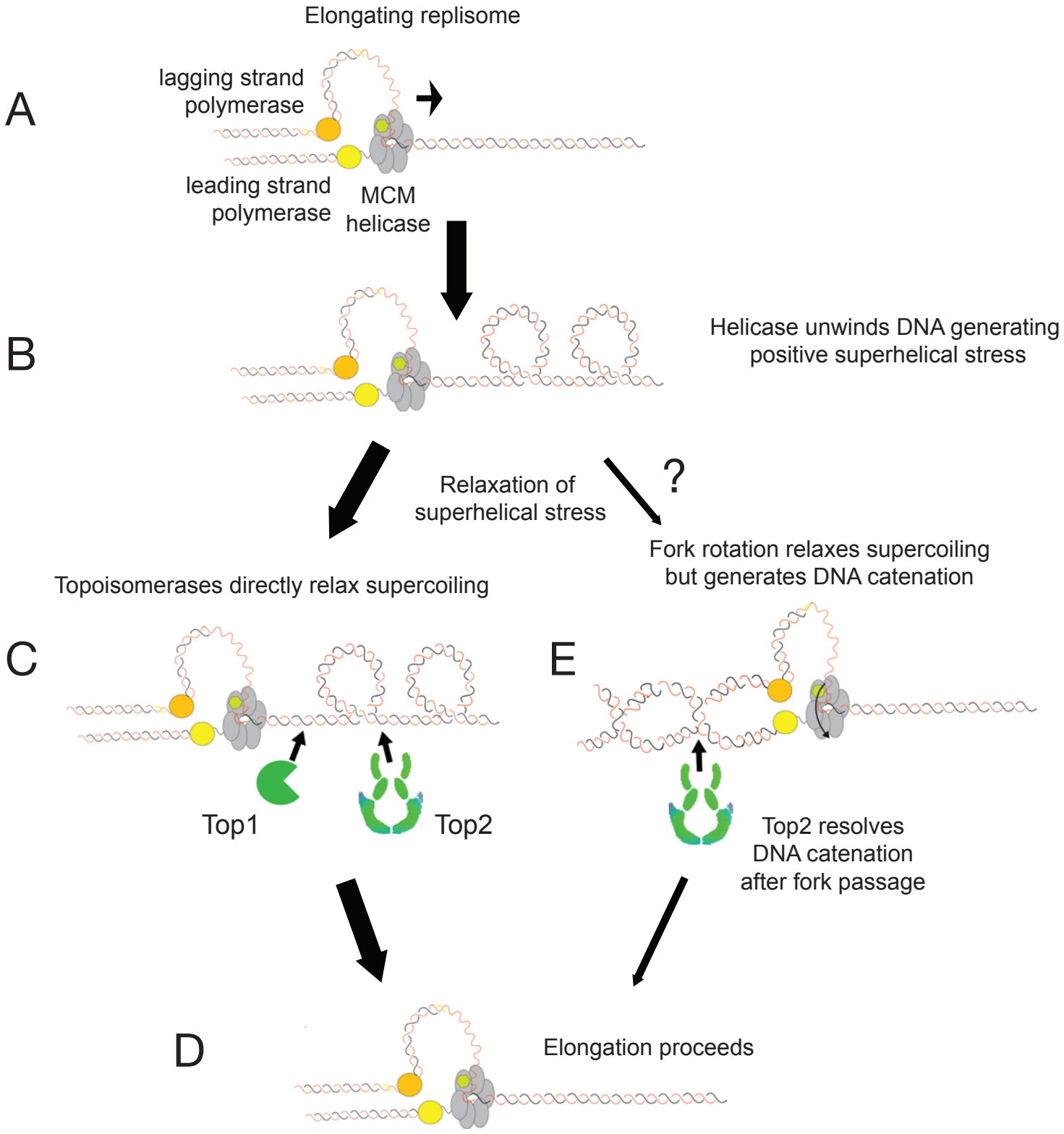

Schalbetter_ Fig.S2

Analysis of replication fork rotation by resolution of individual catenation states and quantification of relative strengths of the signal from each state

Allow plasmids to replicate once in absence of Top2 activity, block in G2 and purify total DNA

Treat with nicking enzyme NbBsmI and resolve products on 2D agarose gels

Quantify signal from each nicked catenated dimer by densitometry, correcting for local background

Indiviual catenated states are not resolvable when they retain supercoiling. Illustrated below in one dimensional analysis of purified DNA.

The first dimension promotes resolution of catenanes with low numbers of intertwines, the second dimension allows resolution of catenanes with high number of intertwines

Quantify signal in a region over each catenated dimer CatAn spot from n=1 to n=27 or 30 (if observable). Also quantify signal in regions covering all CatAn=1 to n=20 and the distribution in a region from ≥ n=21 including all unresolvable CatAn >27 or >30.

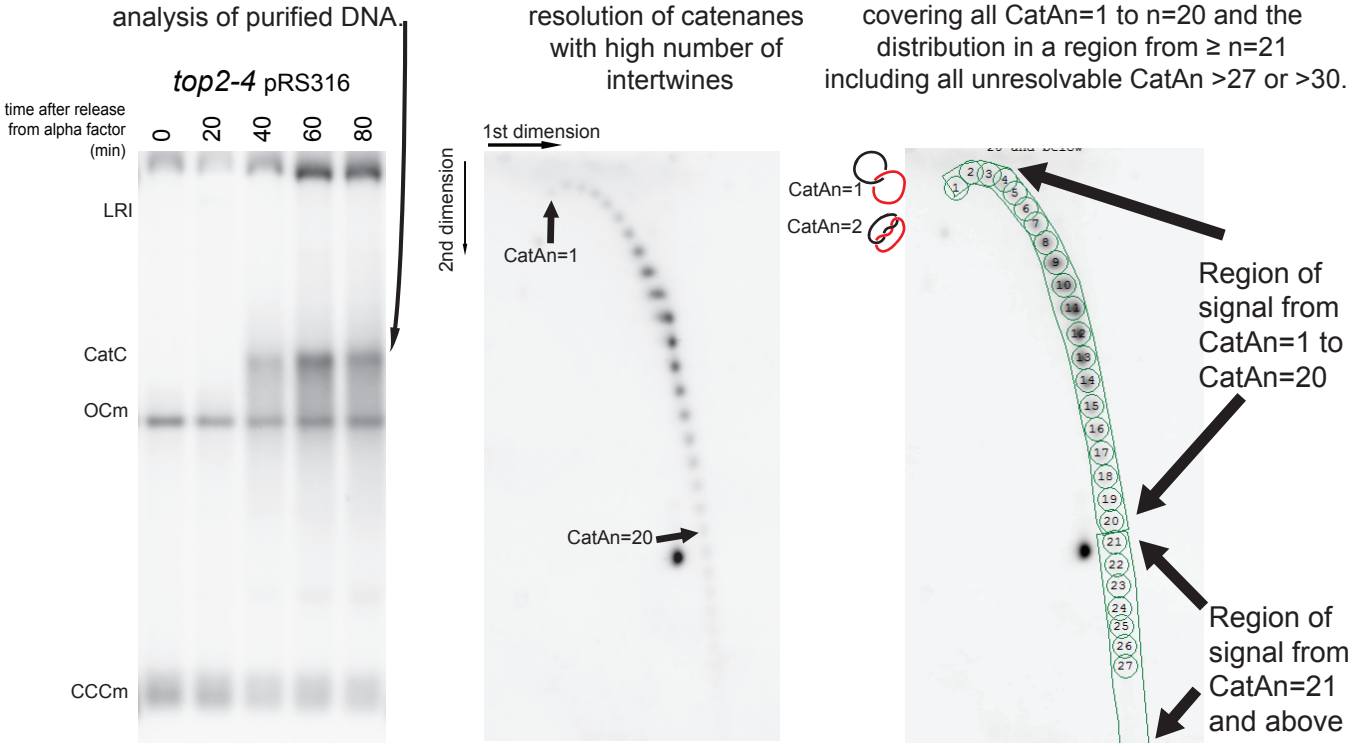

Calculate 1: Relative intensities of all signals associated with region 1 to 27 correcting for background
2: Quantify relative amount of all signal in arc including regions 1 to 20 and 21 and above correcting for background.
3: Calculate median of entire distribution by relating signal in regions 1 to 20 to total signal of large region 1-20 and determining position along arc where 50% of total signal (total signal in regions 1 to 20 and 21 and above) has accumulated.
4. Take average of at least 3 experiments for quantifying differences in DNA catenation of plasmids and at least twice for quantifying differences between different genetic backgrounds (See Table S2 for exact number of replicates for each experiment).

Schalbetter_ Fig. S3

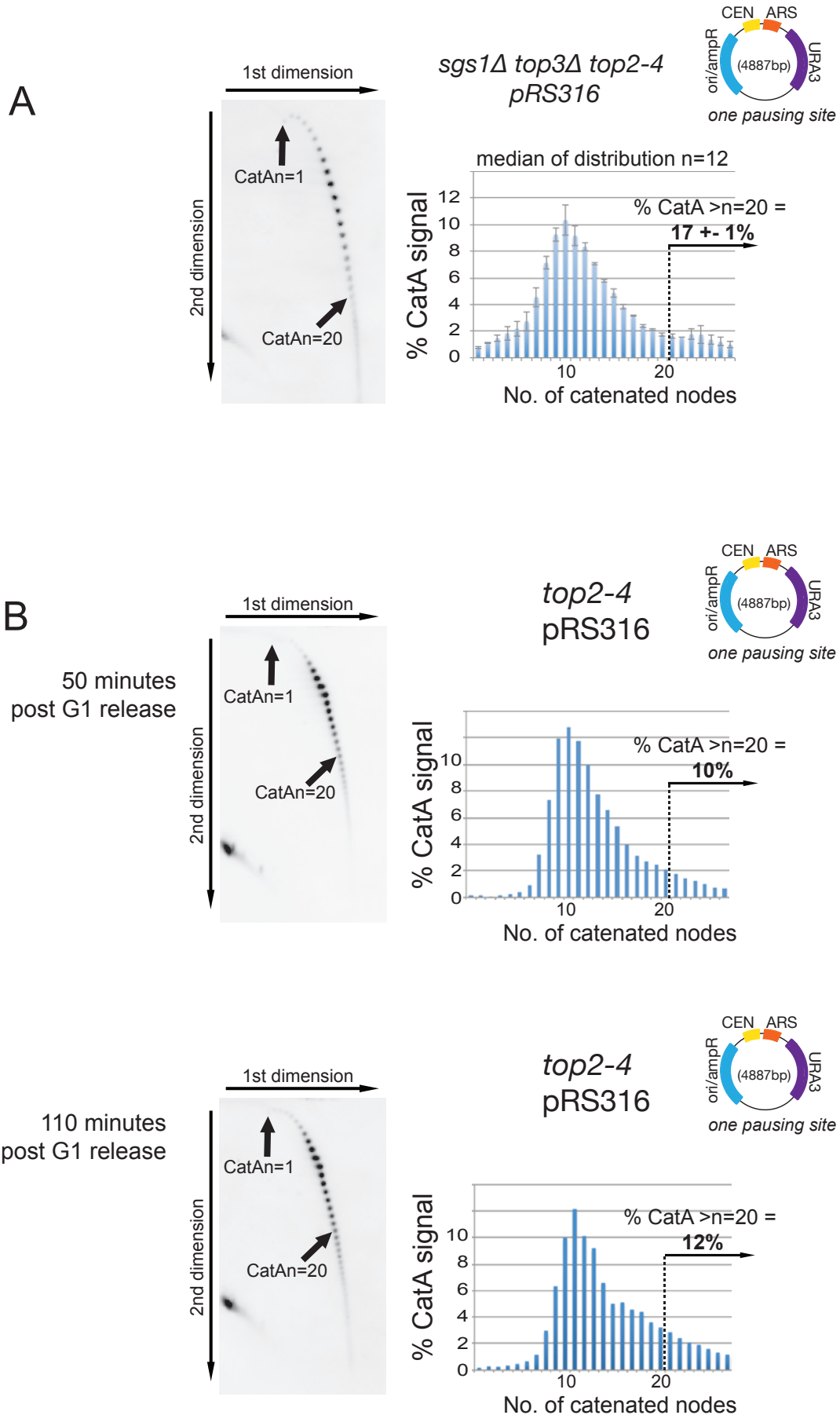

Schalbetter_ Fig. S4

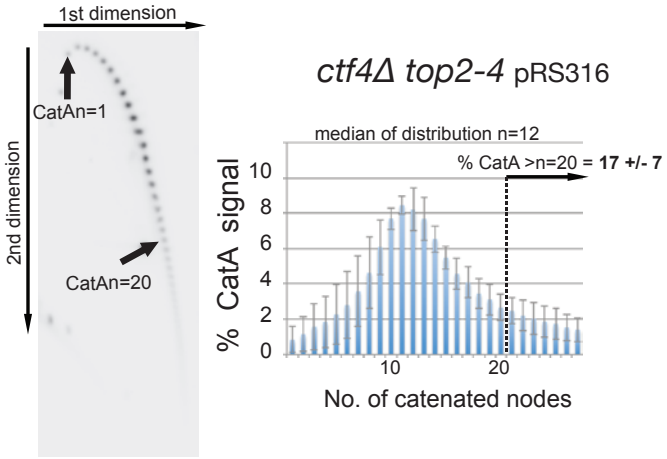

Schalbetter_ Fig. S5

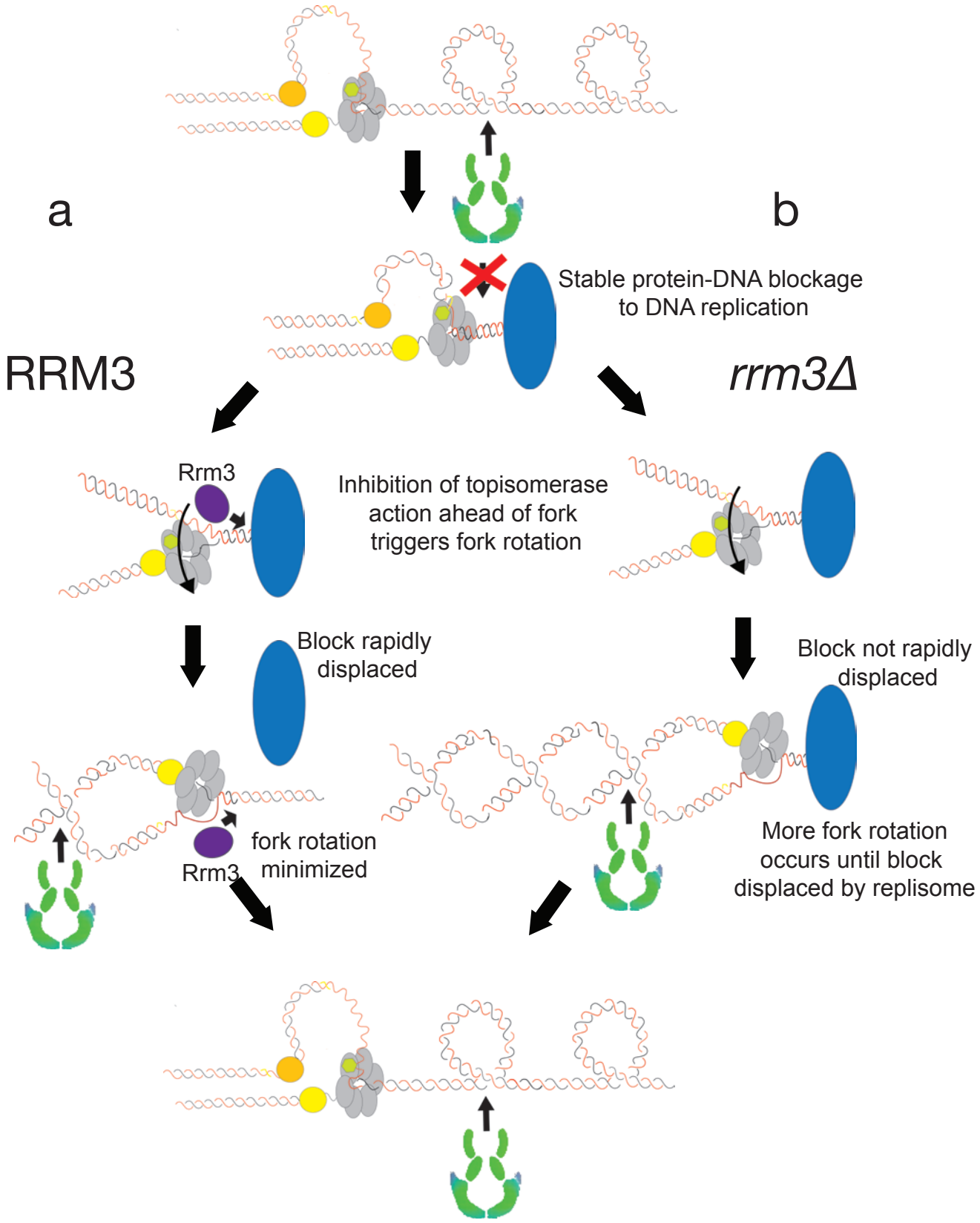

Schalbetter_ Fig.S6

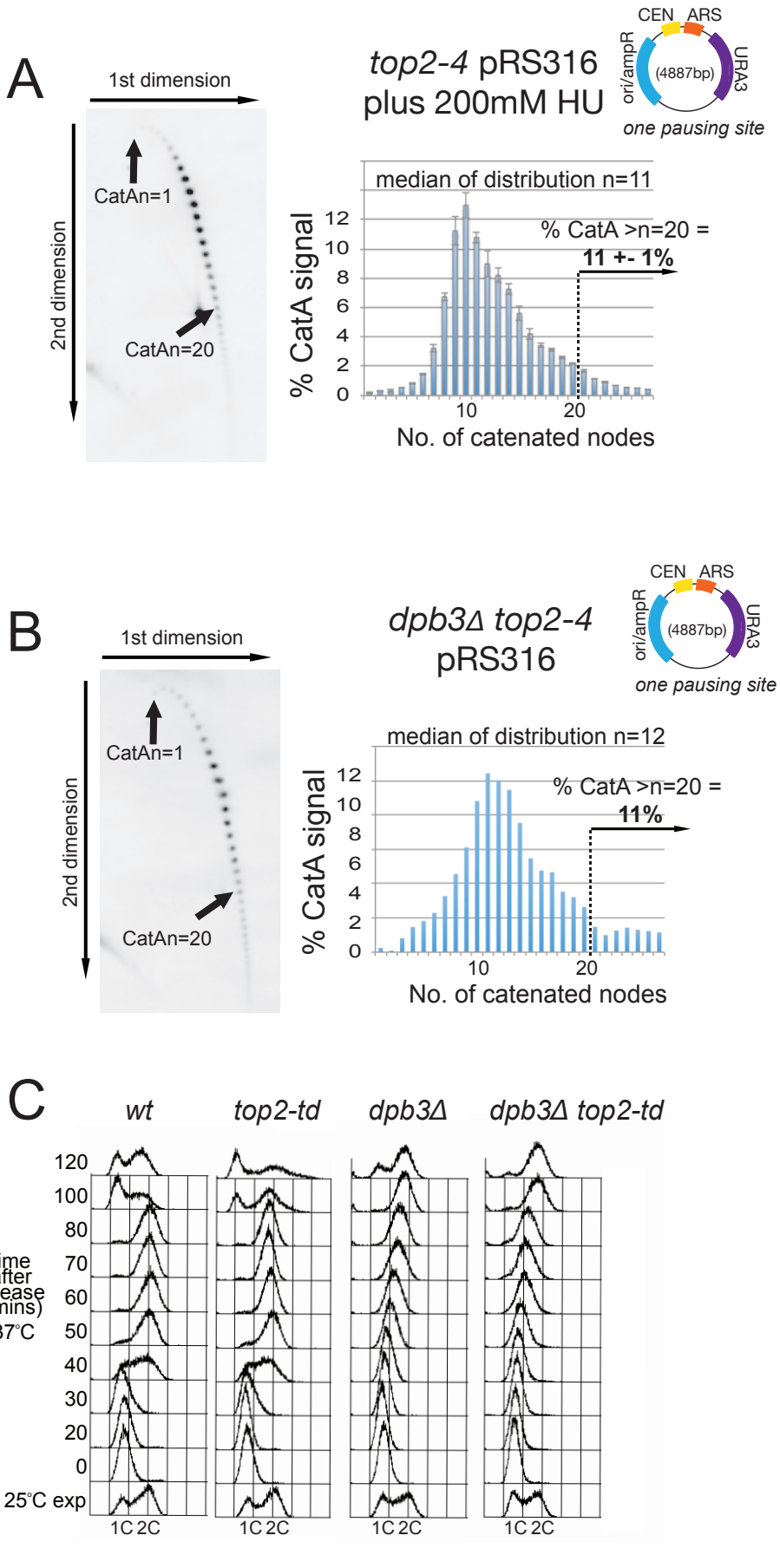

Schalbetter_ Fig.S7

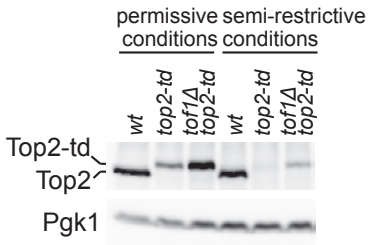

Schalbetter_ Fig.S8

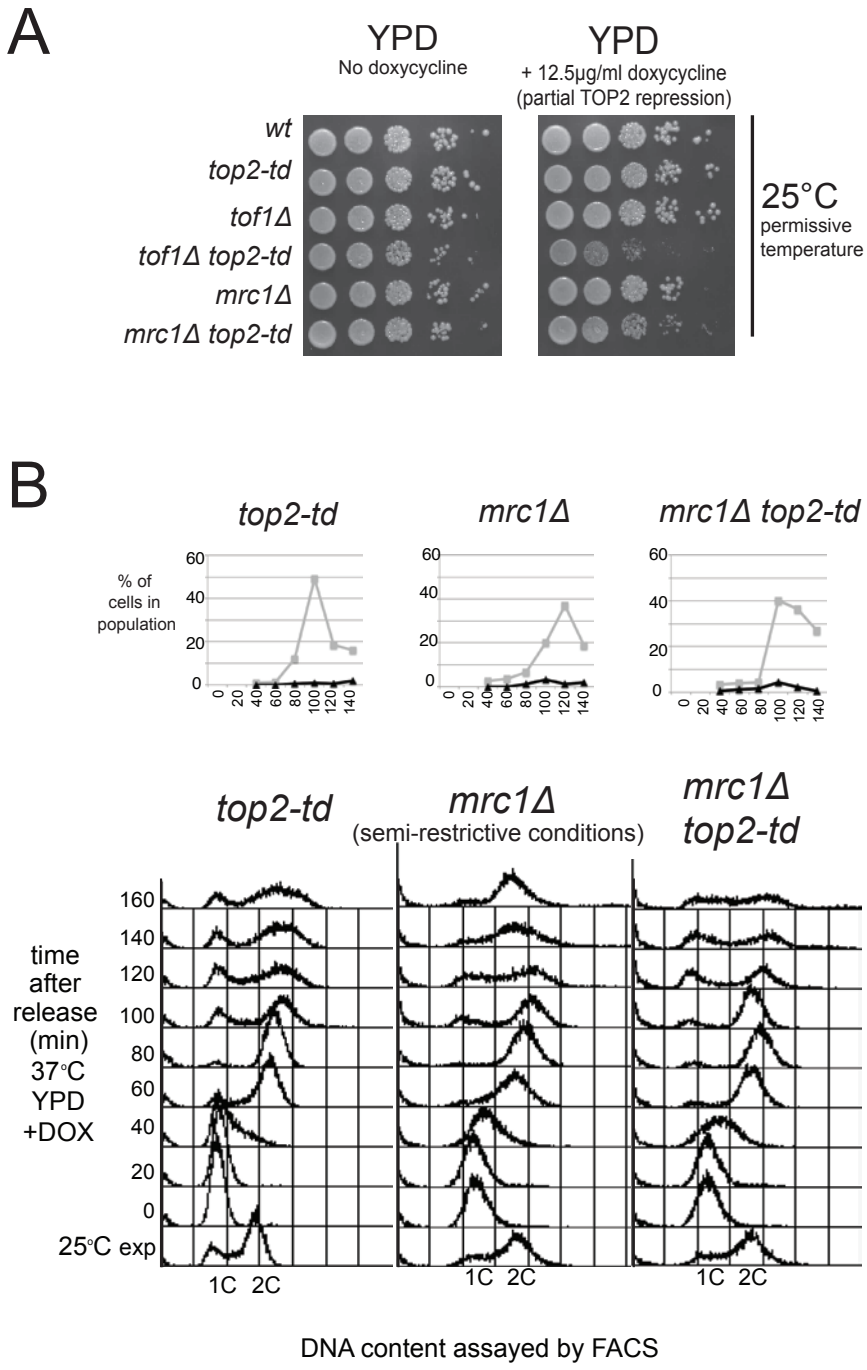

Schalbetter_ Fig.S9